Effects of Averaging Procedures for Electrical Properties at the Interface of Dissimilar Tissues in the Human Head with FDTD Modelling

W. G. Whittow and R. M. Edwards

Department of Electronic and Electrical Engineering Loughborough University, Leics. LE11 3TU

Phone: +44 (0) 1509 227 066

Fax: +44 (0) 1509 227 014

Email: r.m.edwards@lboro.ac.uk and w.g.whittow@lboro.ac.uk

Abstract—The FDTD method builds a problem space out of finite sized Yee cells. The interfaces between heterogeneous materials can be treated in different ways. This paper investigates ways of calculating the effective permittivity and conductivity at dissimilar tissue interfaces. Both homogeneous and anatomically realistic heads are considered. Importantly, this paper finds that whilst the effects of the different averaging techniques are small for homogenous heads they are significant with anatomically realistic heads. The effects are particularly apparent if internal structures in the head are near resonance. The paper shows that the choice of averaging technique has an impact on results and therefore should be explained as a parameter of the simulation technique. Data for 0.9, 1.5 and 1.8 GHz are included here.

Index Terms—FDTD, dielectric interface, averaging, effective permittivity

I. INTRODUCTION

The study of interactions between biological material and the energy generated by personal communications devices is currently topical. The Finite-Difference Time-Domain (FDTD) model is the most common computational tool used to investigate bioelectromagnetics [1]. Two texts on FDTD are [2] [3]. The problem space in the FDTD grid is composed of many Yee cells [4] of finite size, this allows heterogeneous objects of complex shape, such as the human head, to be modelled. The electric and magnetic field components are interwoven in space and lie on the edges of the Yee cell. This results in uncertainties when the field component needs to be calculated at the interface between different materials [5]. Both the conductivity and permittivity at the interface need to be given values to calculate the FDTD equations. Taflove [2] reviewed the area of modelling curved surfaces. This is done by using a volume weighted average of the permittivity and the conductivity in Yee cells which are cut by a dielectric interface. The author of [2] considered this simple technique to be better than simple stair-casing techniques. However, this is generally not possible when applied to an anatomically realistic human head, as the data is only provided in finite size cuboids [6] [7] [8]. This is because the imaging process converts the continuous human body into discrete finite sized voxels of data. Wainwright [9] noted that MRI scans have difficulty distinguishing between two different tissues and a composite material may be used that has intermediate properties.

There is little coverage of the topic of averaging dielectric properties at heterogeneous interfaces in the literature despite there being a vast number of FDTD papers. Many landmark journals [8] [10] [11] [12], that investigate the energy absorbed in the head from a mobile device, do not mention the treatment of inhomogeneous dielectric boundaries.

Several journals have considered the problem of dielectric interfaces between Yee cells and a review of the area shows that different techniques have been considered. Nadobny [13] stated that the averaging of material properties at interfaces between neighbouring media often leads to significant errors. He proposed a post processing method, which approximates the correct field behaviour at the interfaces by interpolating between the calculated FDTD values. The errors have been calculated [14] for different methods of modelling dielectric interfaces, when applied to microwave circuits. Popovic [15] and Celuch-Marcysiak [14] both stated that, at the interface the dielectric properties are often arbitrarily assigned to either material. Zhang [16] concluded that the interface required special treatment and proposed using an effective permittivity calculated as the arithmetic average of the properties of the two materials. Railton [17] and Reineix [18] also used arithmetic averaging of the permittivity for the simple interface of two layers with zero conductivity. Hwang [19] states that three methods of calculating the effective permittivity are in use; arithmetic, geometric and harmonic means. The accuracy of the three techniques depended on the cell size. Hirono [20] also used both arithmetic and harmonic averages of the permittivity at the interface. Again the accuracy depended on the cell size. Hwang [19] and Hirono [20] considered the interface of two dielectric materials when the interface was offset from the edge of the Yee cell. They both considered that the arithmetic mean value of the permittivity should be used for the electric fields tangential to the interface, and the harmonic mean should be used for the electric fields normal to the interface.

The literature generally discusses the averaging of the permittivity, however, there is little mention of the effective conductivity. Although, Marrocco [21] assumed the conductivity could be treated in the same way.

The averaging method at material interfaces is particularly relevant to the modelling of human heads. As the data is generally provided as cuboids of tissue, hence conformal methods of modelling curved surfaces can not usually be used.

The human head is comprised of tissues that have a conductivity, and is therefore more complex than other FDTD applications which model interfaces between objects with zero conductivity. The human head is a complex heterogeneous object comprising many tissues with many different interfaces. Thus, it is particularly important that these interfaces are modelled correctly or at least that the researchers declare which technique has been used.

II. DESCRIPTION OF MODEL

For our comparisons we have used an independent 3D FDTD code has been written; see Taflove [2] for an excellent reference. Perfectly Matched Layers (PML), with geometric grading [22], absorbing boundary conditions are used to terminate the grid. The PML is eight cells thick and is positioned ten cells from the head. The FDTD grid size was 174x140x140 cells in the *X*, *Y*, and *Z* dimensions. The tissues are assumed to be non-magnetic and hence the averaging of the permeability and the magnetic resistivity have not been considered. The ability to change the averaging procedure was critical to these results and therefore commercial software was not used in this work. However the code used here has been fully validated [23].

A. Plane Wave Source Irradiation

A plane wave is injected into the grid using the total field / scattered field approach [2]. This produces a *Z* polarised plane wave propagating in the *X* direction (from the nose to the rear of the head). See Fig. 1 for orientation of the axes. The power density used was 50W/m^2, the maximum permissible exposure limit for controlled environments [24] [25]. This is the power density used in a closely related paper by Hirata [26]. Note that the maximum permissible exposure limit for the general public is 10W/m^2 [24], and results in this paper can be scaled accordingly.

B. The Head Model

A head matrix based on The Visible Human was provided by Brooks Air force [6] was used. The head, which is based on photographs and MRI data, is that of an adult male and has twenty-five tissue types. The data is available at both 1 and 2mm resolutions. This model is popular and has been used by many researchers.

Fig. 1 shows a cross section of the 2mm head, through the centre of the eye. The layers of fat, muscle and skin in front of the eye can be seen which make up the eyelids. The size of the Yee cell was 2mm and equal to the resolution of the head data. The lowest number of cells per wavelength was always greater than ten, and reasonable results have been obtained with only four [27]. Although, the Brooks head is not exactly symmetric, a line of symmetry, in the Y direction, has been included in this model to save memory and computational time. This was achieved by replacing the mid-plane of the grid with a magnetic wall [26], and thus assuming the other half of the head is identical. N.B. Fig. 1 shows the whole head to aid visualisation of the problem. The use of symmetry was found to have negligible effect on SAR results in the eye [23] [28].

The dielectric properties are calculated with aid of the 4-Cole-Cole extrapolation [29] and are frequency dependant. The densities of the different materials are the same as used by Mason [30].

The SAR is calculated with the twelve-field approach as used by Caputa [31]. This method places all the electric field components at the centre of the voxel. Caputa believed that this method was better than the six-component method as the power distribution is defined at the same location as the tissue mass. The six-component method places the electric field components at the corner of eight cells and the conductivity at this point can be either averaged from the eight surrounding cubes or the maximum value can be used [32].

C. Averaging At Dielectric Interfaces

In a 3D FDTD model, a Yee cell is surrounded by twelve electric field components. The cells are homogenously filled. However, the electric field components are calculated at the interface of four different cells. Note. that the E_x, E_y and E_z components are situated on different sides of the Yee cell and the effective properties at these locations are calculated from four different cells. The literature reviewed in Section I, mainly considered applications with an interface between two different media, however, in the human head there are instances where four different tissue voxels meet at the same electric field node. This means that a new effective permittivity and conductivity need to be assigned at each node where the electric fields are calculated. Several different methods of averaging are currently used as outlined in Section I. These are: no averaging (assuming the interface has the properties of one of the neighbouring materials), arithmetic, geometric and harmonic averaging. The formulae for these different averaging techniques are shown below;

Arithmetic mean: $$\varepsilon^* = (\varepsilon_1 + \varepsilon_2 + \varepsilon_3 + \varepsilon_4)/4 \quad (1)$$

Geometric mean: $$\varepsilon^* = \sqrt[4]{(\varepsilon_1 \varepsilon_2 \varepsilon_3 \varepsilon_4)} \quad (2)$$

Harmonic mean: $$\frac{1}{\varepsilon^*} = \frac{1}{4\varepsilon_1} + \frac{1}{4\varepsilon_2} + \frac{1}{4\varepsilon_3} + \frac{1}{4\varepsilon_4} \quad (3)$$

Where ε^* is the new effective permittivity and $\varepsilon_{1,2,3,4}$ is the permittivity in each of the fours cells at the interface. Note that all three formulae give the same answer when the average is taken over four homogenous cells. If the tissues are not homogenous then the arithmetic mean produces the highest value, followed by the geometric mean, while the harmonic mean provides the lowest value of the effective permittivity at the interface of the four heterogeneous Yee cells. The same formulae can be applied to the effective conductivity σ^*. However, at an air / tissue interface, the conductivity of air is zero, and both the geometric and harmonic means do not produce a finite value. Therefore, the air / tissue interface must be treated as a special case for geometric and harmonic averaging techniques. Ten possibilities are considered and are listed in Table 1.

Note that the “No averaging” technique does not use averages of the permittivity or the conductivity for the air / head interface but instead uses the electrical properties of the head at the node at the interface. For the case of the anatomically realistic head, the properties of skin are used at the surface. However, the tissue interfaces inside the anatomical head are more complex, and instead of arbitrarily choosing the electrical properties at the interface from one of the four surrounding Yee cells, the internal effective properties are calculated as the arithmetic mean. Thus, the difference between the “Average” and the “No averaging” techniques is the treatment of the effective properties at the air / head interface.

III. RESULTS

Initially, the different averaging methods were applied to a homogeneous sphere of muscle illuminated by a plane wave at 2.06GHz [33]. The relative permittivity of the sphere was 55.57 and the conductivity was 2.25S/m. The sphere had a diameter of 0.066m. The SAR, into the sphere, is normalized to the input power density and is compared to the Mie series [34]. The results of the different averaging techniques are shown in Fig.2.

The largest SAR value, with all the averaging techniques, is at the centre of the sphere. The order of the maximum SAR (from lowest to highest) is Harmhead, Geohead, Harmhalfskin, No averaging, Geohalfskin, Harmavcon, Geoavcon and the highest SAR is using the Average method. Note, that for the homogenous sphere, Geoavcon and Geopermavcon are the same. As the sphere is homogeneous the only difference in the averaging process is at the surface, this explains why there is little variation in the SAR levels with the different techniques and concludes to maximal ranges of SAR at interfaces between dissimilar materials. Therefore, by applying these techniques we have been able to compare their results with the Mie series that has an exact theoretical value.

Next, the effects of the different averaging techniques were applied to an anatomically realistic head. A $50W/m^2$ plane wave excitation was used as the incident source. The plane wave is travelling in the X direction from the nose to the back of the head. The frequency of excitation is 1.8GHz. At dielectric interfaces, both the permittivity and conductivity are averaged.

Fig.3 shows results of the SAR along the X axis through the centre of the eye. The plots show two peaks, one at the interface between the eyelid and the eye and a larger peak at the centre of the eye, at X=0.018m. The effects of the different averaging techniques are more significant at the second peak at the centre of the eye. Hirata [35] showed that a peak in the SAR at the centre of the eye is due to the eye resonating due to its geometric shape. The centre of the eye is homogenous and is composed of humour, thus the large discrepancy in the range of SAR values at the centre of the eye does not occur at a tissue interface. Different averaging techniques applied to the electrical properties, at the dielectric interfaces, change the resonance of the eye. At the centre of the eye, at X=0.018m, the different averaging techniques investigated in this paper can cause variations in the local SAR of approximately 100%. Thus, the choice of averaging technique is extremely significant when applied to an anatomically realistic head. Since there is no standard for averaging in FDTD, we have chosen to normalise our results to formulation “Average” as shown in table 1. Note that this does not imply normalisation to the mean of the ten methods shown in this paper. Also note that no data exists as to which of the averaging methods is currently the most popular.

Fig.4 shows the SAR through the eye of the Brooks head at 1.8GHz, varying only the averaging of the permittivity. Geometric, harmonic and arithmetic averaging is used for the permittivity. The arithmetic mean is used for all three cases for the conductivity at the dielectric interfaces. Thus, the results in Fig.4 demonstrate the differences to the SAR in the eye when the averaging of the permittivities at the interfaces are varied. The variation in the effective permittivity at tissue interfaces caused changes to the amplitude of the SAR levels in the eyelid. However, there is little variation in the amplitude of the SAR at the centre of the eye. The location of the maximum SAR in the eye is altered, with lower effective permittivity (harmonic) causing the maximum SAR to move closer to the surface of the eye. Fig.4 does not show the large variation in SAR at the centre of the eye found in Fig.3. Therefore, the variation in the SAR in the eye, due to changes in the resonance of the eye, is mainly due to the effective conductivities used at the interfaces and the effective permittivities are less significant.

The results in Fig.3 and Fig.4, show the variation in SAR due to the averaging method applied to an anatomically realistic head. However, these results only show the SAR in individual voxels, and these voxels are very small and are sensitive to change. Table 2 shows results of the SAR averaged over 1g, 10g and over the whole eye. Note the eye in this model has a mass of 8.37g. The 1 and 10g volume averages use cubic volumes of tissue. The range of volume averaged SAR results in Table 2 is less dependent on the averaging technique than the sensitive individual voxel results. However, the changes are still significant. The maximum SAR averaged over 1g varied by 53%, the 10g SAR varied by 64% and the SAR averaged over the eye varied by 58%. For each of the three criteria the highest volume averaged SAR is found when using “Harmavcon”. This uses the harmonic mean to calculate the effective conductivities and permittivities. At the air / tissue interface the effective conductivity is calculated using the arithmetic average of the conductivities of the surrounding cells. Therefore, the highest SAR values were found when the lowest effective conductivity was used. Note, that an averaging technique that produces a higher SAR averaged over 1g, does not necessarily increase the SAR over 10g or averaged over the whole eye. This corroborates the results found in Fig.3 that showed that the averaging technique that produced the highest SAR at the eyelid, did not produce the highest SAR at the centre of the eye.

Further investigations into the different averaging techniques have been applied to the anatomically realistic head at 1.5GHz, the frequency used for mobile devices in Japan. These results are shown in Fig.5. The results are similar to those at 1.8GHz shown in Fig.3. The different averaging techniques cause significant differences to the SAR levels through the centre of the eye. Again, the eye resonates at this frequency and differences to the modelling of the tissue interfaces affect this resonance. The range of SAR at the centre of the eye varied by approximately 100% with the different averaging techniques applied at tissue interfaces.

The results at 0.9GHz are shown in Fig.6. At this frequency, the eye in the model does not resonate and the figure shows that there are two approximately equal peaks, one near the surface of the eye and a second peak at the centre of the eye. Although, the differences due to the different averaging techniques are smaller at this frequency, they are still significant. As the eye is not near resonance, the differences in the modelling of the tissue interfaces are less significant.

IV. CONCLUSIONS

This paper has investigated various possible methods of modelling material interfaces using the FDTD technique. This has been done by assigning effective permittivities and conductivities to the electric field nodes at the tissue interfaces. Results have shown small differences for a homogeneous sphere. However, much larger variations were found when these different effective values were applied to the tissue interfaces of an anatomically accurate human head. The value of the effective conductivity was found to be more significant than the effective permittivity. The effects of modelling the tissue interface may be particularly significant at frequencies when internal structures in the head, such as the eyes, may be resonant, as the resonance is sensitive to changes in the model. Our results indicated that because of resonance changes to boundary conditions manifested themselves in changes to SAR away from the boundary. The effects of modelling the interfaces are particularly apparent when there are large gradients in the tissue properties. The eye is composed of the following layers; cornea (with a conductivity of 1.86S/m at 1.8GHz), lens (1.15S/m) and humor (2.03S/m). The lens has a significantly lower conductivity than both the cornea and the humor. This phenomenon of large variations in the conductivities of adjacent tissues also occurs outside the eye. A typical cross-section into the human head is composed of the following tissues; skin (with a conductivity of 1.19S/m at 1.8GHz), fat

(0.08S/m), muscle (1.34S/m), bone cortical (0.28S/m) and mucous membrane (1.23S/m). Thus, there are many tissue interfaces with relatively steep conductivity gradients.

The largest variation in properties occurs at air / metal interfaces. In FDTD, metal objects can be modelled by forcing the tangential electric field values to zero (PEC) or by setting the conductivity of the Yee cells equal to the conductivity of metal [1] [36]. This technique creates large variations in the conductivity of adjacent materials. However, our results (not included in this paper), have shown that the averaging technique at air / metal interfaces has negligible effect. This is because the conductivity of metal is many orders of magnitude greater than the conductivity of human tissues.

In many situations, which may have few materials, the choice of averaging technique is less important. However, in the human head with many dissimilar tissue interfaces this is not the case. A suitable solution to the problem is to use arithmetic averaging for both the effective conductivities and permittivities. This allows a smooth transition between heterogeneous materials. It also allows consistency between the calculations of the effective conductivity and permittivity. Note, the effective values can be stored in look-up tables and do not need to be recalculated. This means the different averaging techniques cause negligible differences to the computer runtimes.

The SAR equation includes the conductivity and the density of the tissue and the square of the electric field. In this paper, we have calculated the SAR by averaging the12 electric field components that surround the Yee Cell and then using the conductivity and density at the centre of the cell. An alternative approach would be to use the average SAR values calculated at the edges of the grid using the different effective conductivities and densities at the edges of the cell. In heterogeneous bodies these two techniques would produce different results.

V. REFERENCES

[1] Nikita, K.S., M. Cavagnaro, P. Bernardi, N.K. Uzunoglu, S. Pisa, E. Piuzzi, J.N. Sahalos, G.I. Krikelas, J.A. Vaul, P.S. Excell, G. Cerri, S. Chiarandini, R. De Leo, and P. Russo, A study of uncertainties in modeling antenna performance and power absorption in the head of a cellular phone user. IEEE Transactions on Microwave Theory and Techniques, 2000. 48(12): p. 2676-2685.

[2] Taflove, A., Computational electrodynamics. The finite-difference time-domain method. 1995: Artech House, Inc.

[3] Kunz, K., The Finite-difference time-domain method in electromagnetics. 1993.

[4] Yee, K.S., Numerical solution of initial boundary value problems involving Maxwell's equations in isotropic media. IEEE Trans. Antennas and Propagation, 1966. 14: p. 302-307.

[5] Whittow, W.G., Edwards, R. M. The averaging procedure of the electrical properties at the interface of dissimilar tissues in the human head using the FDTD method at 1800MHz. Loughborough Antennas & Propagation Conference. 2005. Loughborough, UK. p. 340-343

[6] Ackerman, M.J, "The Visible Human Project," Proceedings of the IEEE, vol. 86, pp. 504-511, 1998.

[7] Olley, P. and P.S. Excell. Classification of a High-Resolution Voxel Image of a Human Head. 'Voxel Phantom Development', Proceedings of an International Workshop at the National Radiological Protection Board. 1995. Chilton, UK. p. 16-23

[8] Martens, L., J. Demoerloose, D. Dezutter, J. Depoorter, and C. Dewagter, Calculation of the electromagnetic-fields induced in the head of an operator of a cordless telephone. Radio Science, 1995. 30(1): p. 283-290.

[9] Wainwright, P., Thermal effects of radiation from cellular telephones. Physics in Medicine and Biology, 2000. 45: p. 2363-2372.

[10] Tinniswood, A.D., C.M. Furse, and O.P. Gandhi, Computations of SAR distributions for two anatomically based models of the human head using CAD files of commercial telephones and the parallelized FDTD code. IEEE Transactions on Antennas and Propagation, 1998. 46(6): p. 829-833.

[11] Gandhi, O., G. Lazzi, and C.M. Furse, Electromagnetic absorption in the human head and neck for mobile telephones at 835 and 1900MHz. IEEE Trans. Microwave Theory Technology, 1996. 44(10): p. 1884-1897.

[12] Dimbylow, P.J. and S.M. Mann, SAR calculations in an anatomically realistic model of the head for mobile communication transceivers at 900-MHz and 1.8-GHz. Physics in Medicine and Biology, 1994. 39(10): p. 1537-1553.

[13] Nadobny, J., D. Sullivan, D. Wust, M. Seebas, P. Deufflhard, and R. Felix, A high-resolution interpolation at arbitrary interfaces for the FDTD method. IEEE Trans. Microwave Theory Techniques, 1998. 46(11): p. 1759-1766.

[14] Celuch-Marcysiak, M. and W. Gwarek. Higher-order modelling of media interfaces for enhanced FDTD analysis of microwave circuits. Proc. 24th European Microwave Conference. 1994. Cannes, France. p. 1530-1535

[15] Popovic, D. and M. Okoniewski, Effective permittivity at the interface of dispersive dielectrics in FDTD. IEEE Microwave and Wireless Component Letters, 2003. 14(7): p. 265-267.

[16] Zhang, X. and K. Mei, Time-domain finite difference approach to the calculation of the frequency-dependent characteristics of microstrip discontinuities. IEEE Trans. Microwave Theory Techniques, 1988. 36(12): p. 1775-1787.

[17] Railton, C. and J. McGeehan, An analysis of microstip with rectangular and trapezoidal conductor cross sections. IEEE Trans. Microwave Theory Techniques, 1990. 38(8): p. 1017-1022.

[18] Reineix, A. and B. Jecko, Analysis of microstrip patch antennas using finite difference time domain method. IEEE Trans. Antennas and Propagation, 1989. 37(11): p. 1361-1369.

[19] Hwang, K.-P. and A.C. Cangellaris, Effective permittivities for second-order accurate FDTD equations at dielectric interfaces. Ieee Microwave and Wireless Component Letters, 2001. 11(4): p. 158-160.

[20] Hirono, T., Y. Shibata, W. Lui, S. Seki, and Y. Yoshikuni, The second-order condition for the dielectric interface orthogonal to the Yee-lattice axis in the FDTD scheme. IEEE Microwave and Guided Wave Letters, 2000. 10(9): p. 359-361.

[21] Marrocco, G., M. Sabbadini, and F. Bardatti, FDTD Improvement by dielectric subgrid resolution. IEEE Trans. Microwave Theory Techniques, 1998. 46(12): p. 2166-2169.

[22] Berenger, J.P., A perfectly matched layer for the absorption of electromagnetic waves. Journal of Computational Physics, 1994. 114: p. 185-200.

[23] Whittow, W.G. and R.M. Edwards, Applications of a genetic algorithm for identification of maxima in specific absorption rates in the human eye close to perfectly conducting spectacles. IEE Proceedings Science, Measurement & Technology, 2005. 152(3): p. 89-96.

[24] ICNIRP, Guidelines for limiting exposure to time-varying electric, magnetic and electromagnetic fields (up to 300GHz). Health Phys, 1998. 74: p. p. 494-522.

[25] ANSI/IEEE, IEEE standard for safety levels with respect to human exposure to radio frequency fields 3kHz to 300GHz. Standard C95.1-1992, 1992.

[26] Hirata, A., S. Matsuyama, and T. Shiozawa, Temperature rises in the human eye exposed to EM waves in the frequency range 0.6-6 GHz. IEEE Transactions on Electromagnetic Compatibility, 2000. 42(4): p. 386-393.

[27] Dimbylow, P.J. and O.P. Gandhi, Finite-difference time-domain calculations of SAR in a realistic heterogeneous model of the head for plane-wave exposure from 600MHz to 3GHz. Physics in Medicine and Biology, 1991. 36(8): p. 1075-1089.

[28] Whittow, W.G. and R.M. Edwards. Implications for SAR when using a symmetric phantom exposed to RF radiation using the FDTD method. Technical Seminar on Antenna Measurements and SAR (AMS 2004). 2004. Loughborough, UK. p. 67-70

[29] Gabriel, S., R.W. Lau, and C. Gabriel, The dielectric properties of biological materials: 2. Measurements in the frequency range 10Hz to 20GHz. Physics in Medicine and Biology, 1995. 41: p. 2251-2269.

[30] Mason, P.A., W.D. Hurt, T.J. Walters, J.A. D'Andrea, P. Gajsek, K.L. Ryan, D.A. Nelson, K.I. Smith, and J.M. Ziriax, Effects of frequency, permittivity and voxel size on predicted specific absorption rate values in biological tissue during electromagnetic-field exposure. IEEE Trans. Microwave Theory Technology, 2000. 48(11): p. 2050-2058.

[31] Caputa, K., M. Okoniewski, and M.A. Stuchly, An algorithm for computations of the power deposition in human tissue. IEEE Antennas and Propagation Magazine, 1999. 41(4): p. 102-107.

[32] Simon, W., D. Manteuffel, and A. Lauer. New techniques for FDTD calculation of the SAR induced in the human head by wireless communication devices. Loughborough Antennas & Propagation Conference. 2005. Loughborough, UK. p. 328-331

[33] Gajsek, P., T.J. Walters, W.D. Hurt, J.M. Ziriax, D.A. Nelson, and P.A. Mason, Empirical validation of SAR values predicted by FDTD modeling. Bioelectromagnetics, 2002. 23(1): p. 37-48.

[34] Mie, G., Contributions to the optics of diffusing media. Ann Physik, 1908. 25.

[35] Hirata, A. and T. Shiozawa, Correlation of maximum temperature increase and peak SAR in the human head due to handset antennas. IEEE Trans. Microwave Theory Techniques, 2003. 51(7): p. 1834-1840.

[36] Bernardi, P., M. Cavagnaro, and S. Pisa, Evaluation of the SAR distribution in the human head for cellular phones used in a partially closed environment. IEEE Transactions on Electromagnetic Compatibility, 1996. 38(3): p. 357-366.

Dr. W G. Whittow received the B.Sc in physics from The University of Sheffield, U.K in 2000 and his PhD degree in Electronic Engineering also at The University of Sheffield in 2004. He is currently employed as a Research Associate at Loughborough University, UK.

Dr R M. Edwards read in Electronic Engineering with Communications at the University of Sheffield, England and studied for his PhD with the Department's Communications and Radar Group. He is the Director of the Centre for Mobile Communications Research (C4MCR).

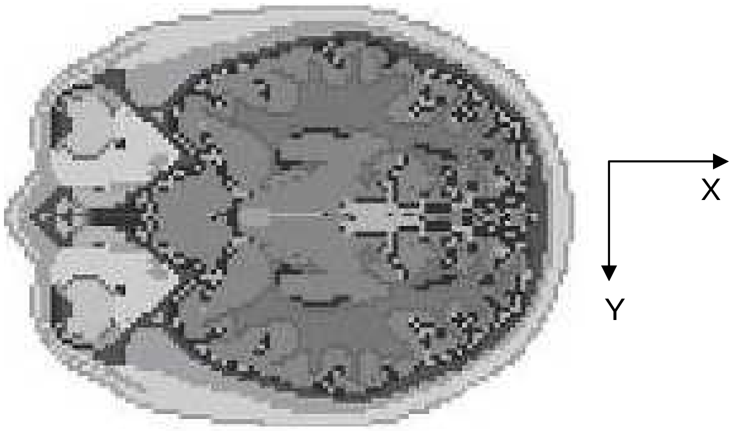

Fig. 1. A cross section through the eyes of the heterogeneous head of 2mm resolution.

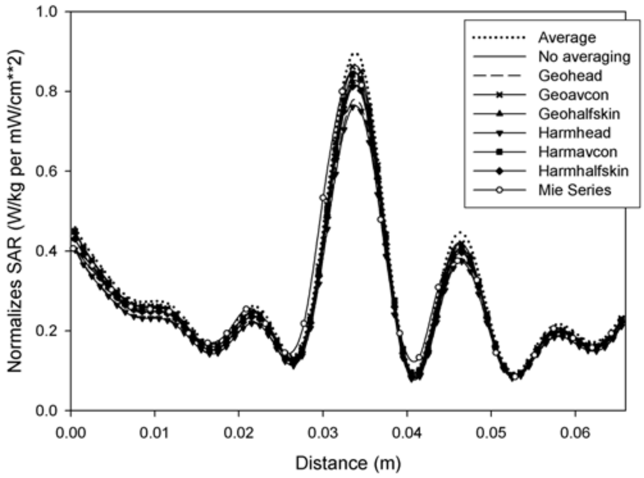

Fig.2. Normalised SAR values across a 0.066m homogeneous sphere of muscle at 2.06GHz. Different averaging techniques are compared to the Mie Series.

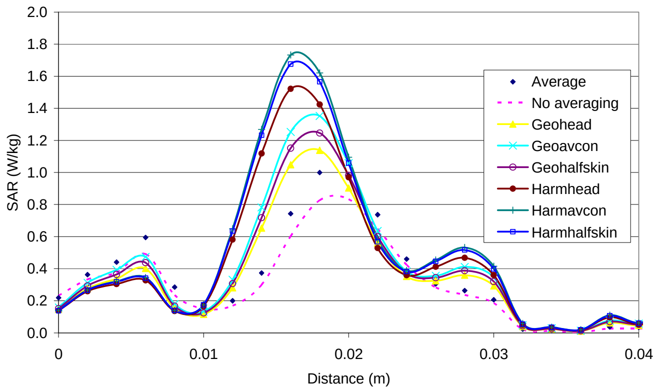

Fig. 3. The SAR through the centre of the eye of the Brooks head at 1.8GHz using different averaging techniques at tissue interfaces. Results are normalised to the maximum of the 'Average' case.

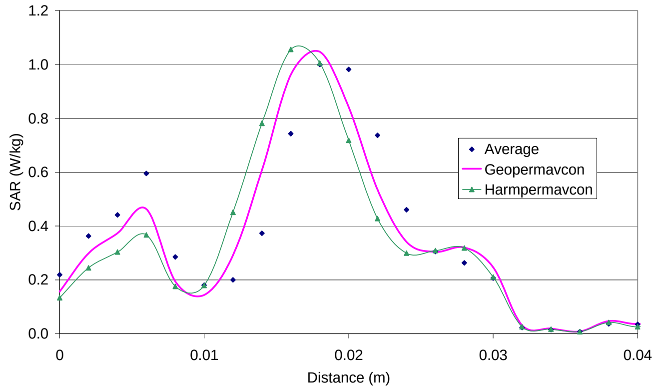

Fig. 4. The SAR through the centre of the eye of the Brooks head at 1.8GHz using different averaging techniques for the effective permittivity at tissue interfaces. Note, the effective conductivity has been calculated using the arithmetic mean of the fours surrounding tissues for all three lines. Results are normalised to the maximum of the 'Average' case.

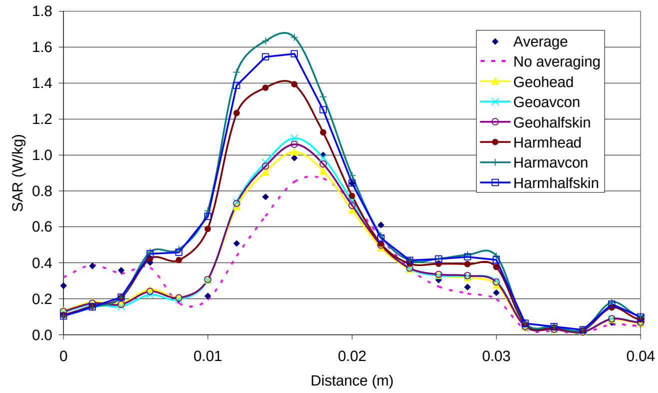

Fig. 5. The SAR through the centre of the eye of the Brooks head at 1.5GHz using different averaging techniques at tissue interfaces. Results are normalised to the maximum of the 'Average' case.

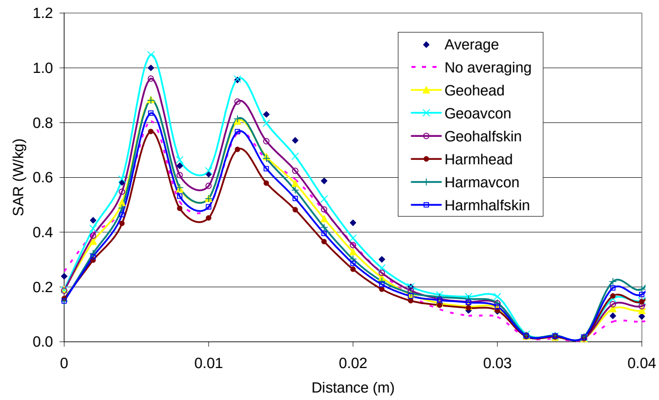

Fig. 6. The SAR through the centre of the eye of the Brooks head at 0.9GHz using different averaging techniques at tissue interfaces. Results are normalised to the maximum of the 'Average' case.

Table 1 . The equation numbers for ten averaging methods in FDTD.

Label	**ε**	**σ**	**σ at surface**
Average	(1)	(1)	(1)
No averaging	(1)	(1)	σ of head or skin ε of head or skin
Geohead	(2)	(2)	(2) using only σ of head tissues not air
Geoavcon	(2)	(2)	(1)
Geohalfskin	(2)	(2)	(2) using $\sigma_{air} = \sigma_{skin}/2$
Geopermavcon	(2)	(1)	(1)
Harmhead	(3)	(3)	(3) using only σ of head tissues not air
Harmavcon	(3)	(3)	(1)
Harmhalfskin	(3)	(3)	(3) using $\sigma_{air} = \sigma_{skin}/2$
Harmpermavcon	(3)	(1)	(1)

Table 2. The maximum SAR averaged over 1g, 10g and the whole eye at 1.8GHz using different techniques for calculating the effective permittivities and conductivities at tissue interfaces. Results are rounded to one significant figure.

	1g SAR (W/kg)	10g SAR (W/kg)	Average SAR in eye (W/kg)
Average	6.4	2.8	1.3
No averaging	6.2	2.6	1.1
Geohead	4.5	2.4	1.3
Geoavcon	6.3	3.0	1.6
Geohalfskin	5.3	2.7	1.5
Geopermavcon	5.6	2.7	1.3
Harmhead	5.6	2.9	1.6
Harmavcon	6.9	3.9	1.8
Harmhalfskin	6.4	3.5	1.7
Harmpermavcon	5.7	3.0	1.1